Localized domain-wall excitations in patterned magnetic dots probed by broadband ferromagnetic resonance

F. G. Aliev,[1,*] A. A. Awad,[1] D. Dieleman,[1] A. Lara,[1] V. Metlushko,[2] and K. Y. Guslienko[3,4]

[1]*Departamento Física de la Materia Condensada, CIII, Universidad Autónoma de Madrid, 28049 Madrid, Spain*

[2]*Department of Electrical & Computer Engineering, University of Illinois at Chicago, Chicago, IL, USA*

[3]*Departamento Física de Materiales, Universidad del País Vasco, 20018 San Sebastian, Spain*

[4]*IKERBASQUE, The Basque Foundation for Science, 48011 Bilbao, Spain*

(Received 5 September 2011; published 4 October 2011)

We investigate the magnetization dynamics in circular Permalloy dots with spatially separated magnetic vortices interconnected by domain walls (double vortex state). We identify a novel type of quasi one-dimensional (1D) localized spin wave modes confined along the domain walls, connecting each of two vortex cores with two edge half-antivortices. Variation of the mode eigenfrequencies with the dot sizes is in quantitative agreement with the developed model, which considers a dipolar origin of the localized 1D spin waves or so-called Winter's magnons [J. M. Winter, Phys. Rev. **124**, 452 (1961)]. These spin waves are analogous to the displacement waves of strings and could be excited in a wide class of patterned magnetic nanostructures possessing domain walls, namely in triangular, square, circular, or elliptic soft magnetic dots.

DOI: 10.1103/PhysRevB.84.144406 PACS number(s): 75.70.Kw, 75.30.Ds, 75.40.Gb

Vortex structures are found in a variety of physical systems, ranging from superfluids and superconductors to tornadoes. As for the single magnetic vortex (SV) state in confined geometry, its first observation already revealed the coexistence of a SV and domain walls (DW), which connect the SV with the vertices of a triangular nanomagnet.[1] Special interest in the confined magnetic vortices is inspired by the possibility of excitation or switching of the vortex core,[2,3] which has been suggested as a potential new road to the creation of nanoscale memory and spin torque vortex oscillators.[4] It is now well established that coexisting vortex-DW configurations are formed in the ground states of magnetic rectangles, triangles, or ellipses,[1,5–7] before the single-domain state appears upon decreasing the particle size.[5] Although excitations of the confined DW or SV states are well understood,[8–12] the nature of the spin waves excited in nanomagnets involving both vortices and domain walls remains unclear. Circular dots are an example of nanomagnets where eigenmodes in the SV ground state can simply be described analytically.[11,13] Decreasing the external magnetic field from saturation, these nanomagnets are known to have two intermediate metastable states: the double magnetic vortex (DMV) and the so-called S state, which is formed by a DW only.[14] Recent reports show that circular magnetic dots with reduced thickness, and therefore enhanced pinning, may accommodate the DMV as a long-living state with two magnetic vortices connected via a DW to edge localized antivortices (AV).[14–17]

Circular dots provide a unique opportunity to investigate the spin wave dynamics of both the vortex-DW (DMV) and SV configurations by reducing or increasing the external magnetic field below or above the vortex nucleation field, H_n. In this system, the vortex cores can be pinned by microstructure related defects, intergrain boundaries, etc.,[18] thereby trapping the system in the metastable DMV state. Provided the perturbation is small enough, the dot can stay in the DMV state for at least the duration of the measurements. We show here that for low fields the magnetization dynamics of circular Py dots with a diameter of 1000 nm and a thickness below 25 nm corresponds to DMV state excitations. The first few lowest-frequency spin wave modes present the first example of confined (standing) quasi-1D spin waves localized along domain walls pinned between the vortex and half-antivortex cores.

For the experiments, a vector network analyzer (VNA-FMR) was used to conduct broadband measurements of the magnetization dynamics in the square arrays of Permalloy dots with spacing between dot edges exceeding the dot diameter in order to avoid influence of the interdot dipolar interaction. We excited the dots by applying small (0.1 Oe) in-plane driving fields created by a coplanar waveguide (CPW), parallel to the magnetic bias field (see the coordinate system XYZ and corresponding indications in Fig. 1). This technique ensures small precession amplitudes of the magnetization around the effective field. In this experimental scheme (see also the sketch in Ref. 19 indicating the directions of the CPW and exciting magnetic field), the rf drive field along X axis excites mainly small in-plane deviations (ΔM_X; ΔM_Y) of nonuniform in-plane magnetization **M**. Small out-of-plane rf field components, created in the waveguide due to finite size of the central conductor, could also excite the magnetization component perpendicular to the dot plane ΔM_Z.[13] The data were analyzed on the basis of the transmission model, under the assumption that the dominant CPW mode is a transverse electromagnetic (TEM) mode and by neglecting the effect of reflection.[19]

In the experiments, we investigated the evolution of the broadband dynamic response of the dot as a function of a slowly changing in-plane bias magnetic field. We first saturate the sample by applying a positive field that is two times larger than the positive vortex annihilation field (H_a). Subsequently, we slowly sweep the field downwards, lowering it past the vortex nucleation field (H_n), and after changing the field polarity, we end at the negative vortex annihilation field. The microwave field drive, parallel to the external bias field, with an amplitude in several thousand times smaller than H_a, mainly couples to DW where the exchange energy is the highest. This permits precise detection of possible localized excitations in the DW.[19] We investigated circular dots with the thicknesses

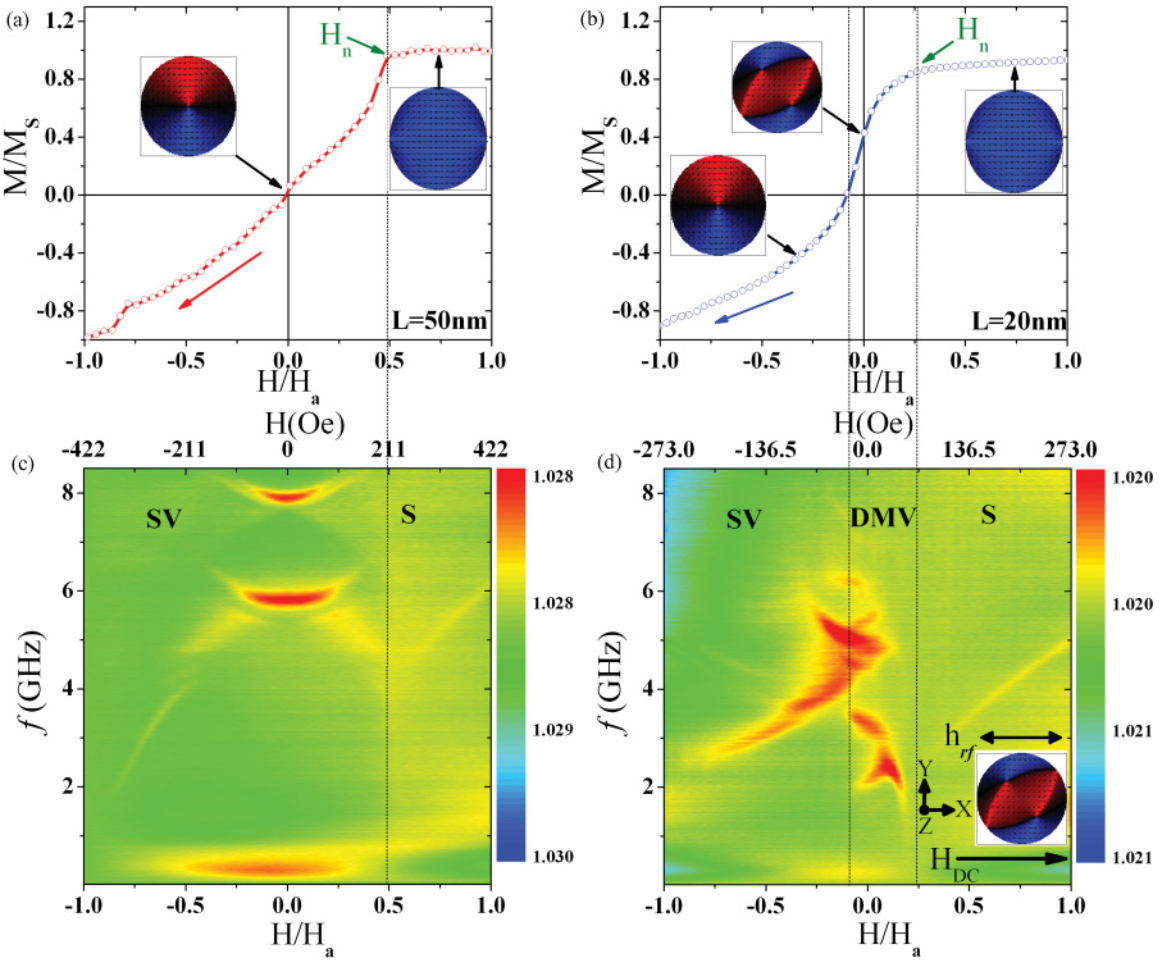

FIG. 1. (Color online) (a) and (b) The static magnetization of the Py dots with 1000-nm diameter and thicknesses of 50 and 20 nm, respectively, measured by sweeping the field from H_a to $-H_a$. (c) and (d) Intensity plots of the measured spin excitation spectra for the Py dot arrays with the bias field swept down from saturation and the driving field applied parallel to the bias field. The magnetic field is normalized by the vortex annihilation field H_a. The vortex nucleation fields are marked as H_n; inserts and vertical lines indicate the saturated S, DMV, and SV magnetic states.

$L = 50$, 25, 20, and 15 nm with diameter $2R = 1035$ nm and 20-nm-thick dots with $2R = 570$ nm. The micromagnetic simulations were carried out using OOMMF code[20] for circular Py dots with a diameter of 1035 nm and thickness of 20 nm, with simulated cell size $5 \times 5 \times 20$ nm^3, $\gamma/2\pi = 2.96$ MHz/Oe, the exchange stiffness constant $A = 1.4 \times 10^{-11}$ J/m, and the Gilbert damping constant $\alpha = 0.01$. We first saturate the dot, using an in-plane field of 1000 Oe. After releasing the field in one step to zero, in agreement with Ref. 14, the dot relaxes by means of two clearly defined steps that have a slope of energy vs time of almost zero (not shown). These steps are two metastable magnetic states which we identify as first the S state and afterwards the DMV state. For our simulations, these states remain stable for about 10 ns only. This can be attributed to the fact that we neglected the magnetic anisotropy and all the imperfections that the real samples usually have. To excite magnetization dynamics, a variable driving field (Gaussian field pulse) with the amplitude of 1 Oe and full width at half maximum (FWHM) of 1 ps was applied. We perform local Fourier transforms over all simulation cells and average these spectra to obtain the spin eigenfrequencies.

Figure 1 compares the static magnetization and dynamic response for dots with thicknesses $L = 50$ nm (left) and 20 nm (right). The spin wave resonances in 50-nm-thick dots for bias fields below the vortex nucleation field $|H_n|$ correspond to the azimuthal modes[19] and are symmetric with respect to the field direction, as expected for the SV state [Figs. 1(a) and 1(c)]. However, this low field response drastically changes for the Py dots with smaller L. Starting from 25 nm, the magnetization dynamics becomes asymmetric at low fields [Fig. 1(d)]. Besides, we find for a parallel excitation field and for bias fields just below H_n several additional peaks with frequencies between 2 and 5 GHz, which are lower than the first azimuthal mode frequency of the SV state, but much higher than the vortex gyrotropic frequency.[6] We claim that these surprising spectra originate from another intermediate state. Namely, we consider that the Py dots in the array are in a metastable DMV state in the field interval indicated by vertical dashed lines in Fig. 1. A reduction of the vortex core

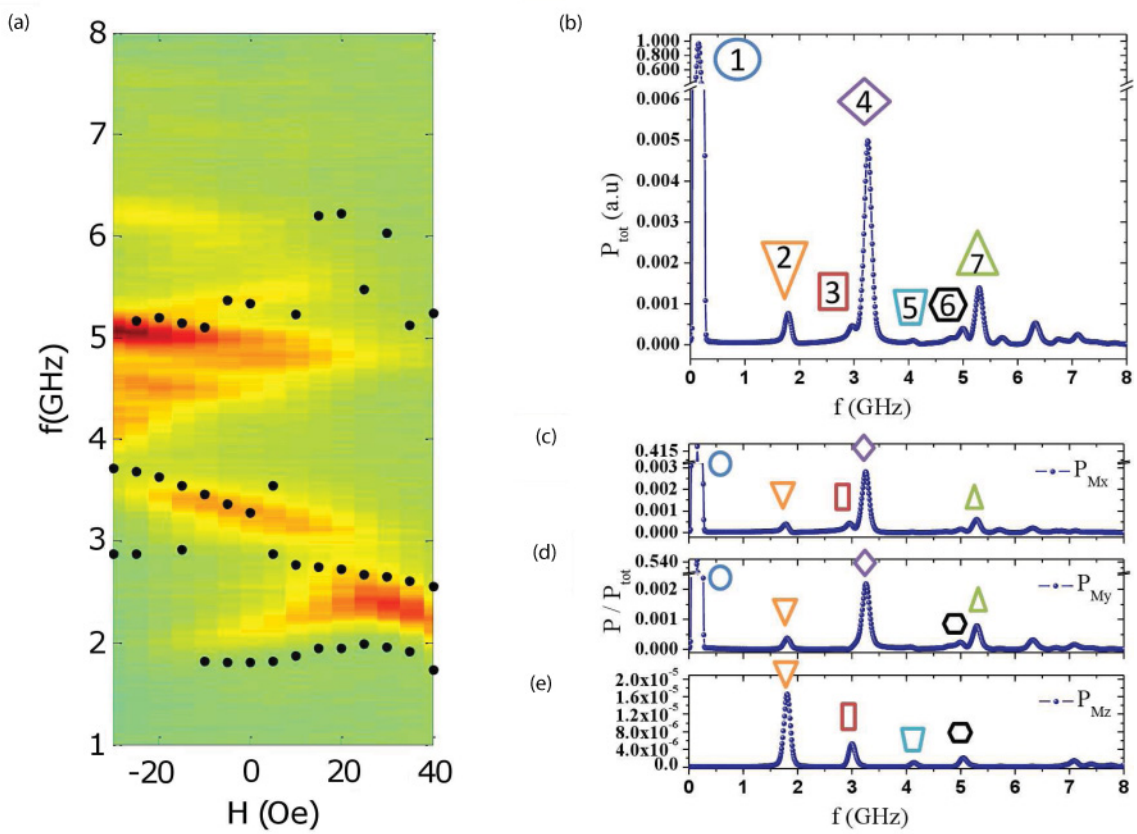

FIG. 2. (Color online) (a) Comparison of the simulations (closed circles) with the experiments [background, see marked part of Fig. 1(d)]. The simulated frequencies are obtained by taking the three strongest peaks at each applied field. (b) Simulated spectrum at zero field for all the magnetization components combined and for (c) M_X, (d) M_Y, and (e) M_Z separately. In (b), the measured intensity peaks are marked by integers, corresponding to the first seven excited spin eigenmodes (see Fig. 3 for the spatial distributions of these modes). The dot sizes for both the simulations and experiment are $2R = 1035$ nm and $L = 20$ nm.

size and a decrease in the dot thickness,[21] accompanied by the enhancement of the effective damping, may be an origin of the stabilization of the metastable DMV state for the thinner dots, in agreement with the previous measurements.[14–17]

In order to investigate the possible metastable states of the dots, we performed micromagnetic simulations. We identified the measured asymmetric eigenmodes [Fig. 1(d)] by comparison of the calculated spin excitation spectra for different metastable (S or DMV) states with the experimental results. Comparison of the dynamic simulations for the S state and DMV states with experimental data reveals that the spin wave modes excited between the positive H_n and small negative bias fields are close to those expected for the DMV state (Fig. 2). It can be seen that the M_X, M_Y and M_Z magnetization components do not respond in the same way to a given field pulse along X direction because of difference in the spatially averaged magnetization. Due to finite size of CPW, combining these three spectra should mimic the experiment more adequately [Figs. 2(b)–(e)]. The robustness of the dynamic response (not shown) further confirms that the detected spin waves are due to the DMV state. Figure 2(a) shows the three strongest peaks (above the gyrotropic frequency) of the simulated spectra compared to the experiments. Clearly, there is a good match between the experiments and simulations.

In order to get more insight into the spin dynamics in the DMV state, we investigate the spatial distribution of the main eigenmodes. Knowing the local distribution of the phases and amplitudes for every cell for a selected eigenfrequency, we can reconstruct the eigenmode profiles.[22] Figure 3 identifies the main eigenmodes excited in the DMV state at zero applied field. The modes are numbered according to the spectra in Fig. 2(b). The first eigenmode is primarily a gyrotropic-mode-type excitation of the vortex cores. Modes 2, 3, 4, and 5 are localized along the domain walls that connect the vortex cores (VC) and edge localized half-antivortex cores. Mode 2 is of an optical type (the different DW's connecting the V-AV-V-AV rhomb apexes are oscillating out of phase) and is localized closer to the dot's edge at the ends of the DWs. Mode 3 shows a node in the oscillation amplitude. Mode 4 (acoustic) reveals no nodes but a strong pinning at the AV positions near the dot edges. Eigenmode 5 is a running wave along V-AV-V-AV rhomb. The higher frequency modes 6 and 7 show strong features localized outside the domain walls. In the supplementary material,[23] we provide time sequences of the variation of the M_X component of magnetization corresponding to the spin wave mode 2 (at 1.8 GHz), mode 3 (2.9 GHz), and mode 4 (3.2 GHz) for the 1035×20 nm Py dot shown in Fig. 3. The time evolution of the magnetization for these modes was obtained in the absence of bias field. While

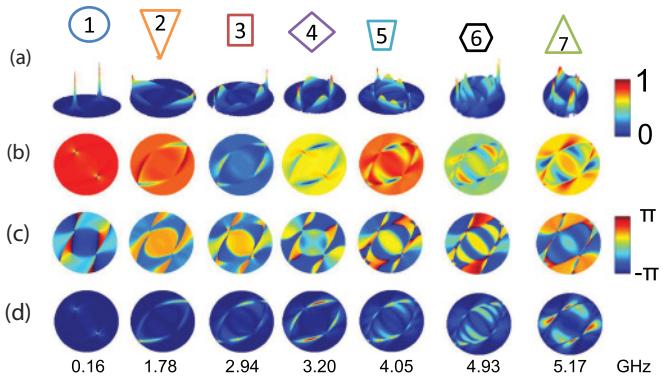

FIG. 3. (Color online) The spatial distributions of the first seven spin eigenmodes at zero bias field corresponding to the frequency spectra of Fig. 2. The snapshots for the relative magnetization ΔM_x component are as follows: (a) 3D-visualization of modulus (a.u.), (b) the real part (a.u.), (c) the phase, and (d) 2D-visualization of the amplitude (a.u.). The dot sizes are $2R = 1035$ nm and $L = 20$ nm. The supplementary material (Ref. 23) shows online 3D animations of the eigenmodes 2, 3, and 4.

mode 2 weakly excites the vortex cores motion, mode 4 does not excite edge half-antivortex. Mode 3 excites motion of both the vortex cores and edge half-antivortices.

We note that in the case of the SV excitations in square dots,[7] the VC is a crossing of the four 90° DWs connecting the core and the square corners. The VC position oscillations then correspond to the change of the DW shape (DW bulging) and length. The VC mode and DW bulging modes are naturally coupled and have the same oscillation eigenfrequency (230 MHz in Ref. 7). These bulging DW modes are essentially different from the considered DW flexural modes, having eigenfrequencies about 2 GHz and higher.

There are two branches of the spin excitations in the presence of a DW: free spin waves with excitations resembling those in an infinite uniformly magnetized ferromagnet, and wall-bounded spin excitations or Winter's magnons,[24] representing oscillations of the DW shape about the static equilibrium position, which can be described as a plane. The DW displacement waves are analogous to the displacements that can propagate along elastic strings (e.g. violin strings) and to the capillary waves on the surface of liquids. The Winter's magnons were considered for the Bloch type of the DW[24] in an infinite ferromagnet. But in our case of the flat soft magnetic dots, the spins lie in the dot plane (xOy) due to strong magnetostatic energy, and a Néel DW should be considered as a ground state. To understand 1D spin waves confined along the Néel DW that is pinned by the V(AV) cores, we determine spin excitations of the wall applying the approach by Slonczewski.[25] To describe the magnetization dynamics, we use the Landau–Lifshitz equation of motion of the reduced magnetization $\mathbf{m} = \mathbf{M}/M_s$ ($|\mathbf{M}| = M_s$ is the saturation magnetization). We assume that there is a Néel DW connecting the V and AV centers (Oy axis) and consider its excitations expressing $\mathbf{m}$ as a sum $\mathbf{m} = \mathbf{m}_0 + \delta\mathbf{m}$ of the DW static magnetization and spin wave contribution. The Cartesian components of the reduced magnetization $\mathbf{m}$ [the Oz axis is directed perpendicularly to the dot plane coinciding with the OZ axis indicated in Fig. 1(d)] are defined by the spherical angles (Θ, Φ): $m_x + im_y = \sin\Theta \exp(i\Phi)$, $m_z = \cos\Theta$. Here, ($\pi/2$, Φ_0) are the spherical angles of the DW ground state $\mathbf{m}_0$. Taking into account that the DW length Δ is about the dot radius R and the dot is thin ($L \ll R$), we neglect the magnetization dependence on the z coordinate and apply for the static DW description an infinite film 1D ansatz $\cos\Phi_0(x) = \sec h(x/\delta)$, $\sin\Phi_0(x) = \tanh(x/\delta)$, where δ is the DW width. Then, introducing the traveling wave ansatz substitution $\mathbf{m}(x, y, t) \to \mathbf{m}_0[x - q(y, t)]$ we consider oscillations of the DW shape writing coupled equations of motion for the DW displacement from its rest position $q(y, t)$ and the magnetization deviation angle ϑ from the dot plane xOy ($\Theta = \pi/2 + \vartheta$). The variables q and ϑ describe flexural modes of the DW or so called Winter's magnons.[24] We introduce a strong pinning near the VC position in the DW ($y = 0$) and no pinning or a strong pinning near the AV core ($y = \Delta$, $\Delta \approx R$). To satisfy these boundary conditions, we use the plane wave eigenfunctions $q_n(y) \propto \sin(k_n y)$, with discrete $k_n = (2n - 1)\pi/2\Delta$ or $k_n = n\pi/\Delta$, $n = 1, 2, \ldots$, respectively, and consider the quantized frequencies of the Winter's magnons $\omega_n = \omega(k_n)$. The magnon frequencies $\omega_n^2/\omega_M^2 = p\int_0^\infty x \sinh^{-1}(\pi x)(\sqrt{x^2 + k_n^2\delta^2} - x)dx + (4/\pi) \times \exp(-\Delta/\delta)$, where $p = L/\delta$, $k_n L < 1$, are calculated from the linearized equations of motion of the variables q and ϑ within the magnetostatic approximation following the method suggested by Guslienko *et al.*[26] They are in good agreement with the measured eigenfrequencies (here $\omega_M = 4\pi\gamma M_s$, γ is the gyromagnetic ratio). Applicability of the model is confirmed by considering variation of the eigenfrequencies for the spin modes 2 and 4 with the dot aspect ratio L/R (Fig. 4). The Winter's magnon eigenfrequencies are $\omega_n \propto \sqrt{L/R}$ at $L/R \ll 1$ similarly to the frequencies of the magnetostatic radial and azimuthal spin waves in the flux closure single vortex state.[27] But for the Winter's magnons, there is a small gap in the spectrum $\omega(k)$ at $k \to 0$ determined by the ratio Δ/δ, reflecting finite dot in-plane size of the more complicated DMV magnetization state.

In conclusion, we identify quasi-one-dimensional (1D) localized spin wave modes confined along the domain walls, connecting vortex cores with half-antivortices in circular magnetic dots. The frequencies measured by broadband

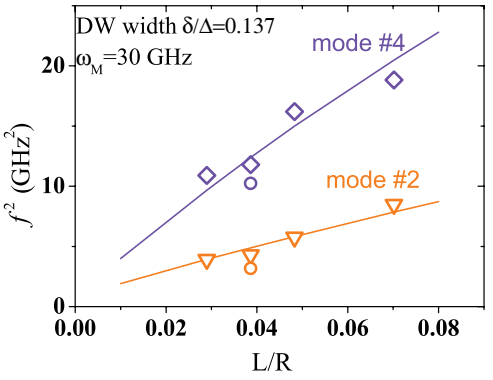

FIG. 4. (Color online) Comparison of the experimental (squares and triangles), analytical (lines), and simulated (circles) eigenfrequencies for the most intensive excited spin modes 2 and 4 as a function of the dot aspect ratio (thickness over radius).

ferromagnetic resonance are in good agreement with the DW flexural oscillation frequencies calculated in the magnetostatic approximation assuming Néel domain walls connecting the vortex and antivortex cores. In general, similar spin waves would be excited by spin torque or microwave magnetic field in thin arbitrary shaped (circular, triangular, rectangular, etc.) patterned magnetic nanostructures possessing magnetic domain walls. Besides, our findings may contribute to the understanding of domain wall motion in magnetic stripes and rings induced by magnetic field or spin polarized current.[28] Finally, our results introduce a scheme to investigate the high-frequency magnetization dynamics of symmetry-breaking states in highly symmetric patterned magnetic elements.

ACKNOWLEDGMENTS

This paper was supported by Spanish MICINN (MAT2009-10139, Consolider CSD2007-00010), CM (P2009/MAT-1726) and SVORTEX (CCC-UAM) grants. K.G. acknowledges support by IKERBASQUE (the Basque Foundation for Science) and by the Spanish MICINN grants FIS2010-20979-C02-01 and PIB2010US-00153. V.M. acknowledges funding from US NSF, Grant No. ECCS-0823813.

*Corresponding author: farkhad.aliev@uam.es

[1] A. Tonomura, T. Matsuda, J. Endo, T. Arii, and K. Mihama, Phys. Rev. Lett. **44**, 1430 (1980).
[2] K. Yamada, S. Kasai, Y. Nakatani, K. Kobayashi1, H. Kohno, A. Thiaville, and T. Ono, Nat. Mater. **6**, 269 (2007).
[3] B. Van Waeyenberge, A. Puzic, H. Stoll, K. W. Chou, T. Tyliszczak, R. Hertel, M. Fähnle, H. Brückl, K. Rott, G. Reiss, I. Neudecker, D. Weiss, C. H. Back, and G. Schütz, Nature **444**, 461 (2006).
[4] A. Dussaux, B. Georges, J. Grollier, V. Cros, A. V. Khvalkovskiy, A. Fukushima, M. Konoto, H. Kubota, K. Yakushiji, S. Yuasa, K. A. Zvezdin, K. Ando, and A. Fert, Nature Comm. **1**, 1 (2010).
[5] M. Hehn, K. Ounadjela, J. P. Bucher, F. Rousseaux, D. Decanini, B. Bartenlian, and C. Chappert, Science **272**, 1782 (1996).
[6] K. S. Buchanan, P. E. Roy, M. Grimsditch, F. Y. Fradin, K. Guslienko, S. D. Bader, and V. Novosad, Nature Phys. **1**, 172 (2005).
[7] J. Raabe, C. Quitmann, C. H. Back, F. Nolting, S. Johnson, and C. Buehler, Phys Rev. Lett. **94**, 217204 (2005).
[8] E. Saitoh, H. Miyajima, T. Yamaoka, and G. Tatara, Nature **432**, 203 (2004).
[9] L. Thomas, M. Hayashi, X. Jiang, R. Moriya, C. Rettner, and S. S. P. Parkin, Nature **443**, 197 (2006).
[10] D. Bedau, M. Kläui, S. Krzyk, U. Rüdiger, G. Faini, and L. Vila, Phys. Rev. Lett. **99**, 146601 (2007).
[11] K. Guslienko, B. A. Ivanov, V. Novosad, Y. Otani, H. Shima, and K. Fukamichi, J. Appl. Phys. **91**, 8037 (2002).
[12] M. Buess, R. Höllinger, T. Haug, K. Perzlmaier, U. Krey, D. Pescia, M. R. Scheinfein, D. Weiss, and C. H. Back, Phys. Rev. Lett. **93**, 077207 (2004).
[13] A. A. Awad, K. Y. Guslienko, J. F. Sierra, G. N. Kakazei, V. Metlushko, and F. G. Aliev, Appl. Phys. Lett. **96**, 012503 (2010).
[14] C. A. F. Vaz, M. Kläui, L. J. Heyderman, C. David, F. Nolting, and J. A. C. Bland, Phys. Rev. B **72**, 224426 (2005).
[15] T. Pokhil, D. Song, and J. Nowak, J. Appl. Phys. **87**, 6319 (2000).
[16] M. Rahm, M. Schneider, J. Biberger, R. Pulwey, J. Zweck, D. Weiss, and V. Umansky, Appl. Phys. Lett. **82**, 4110 (2003).
[17] I. Prejbeanu, M. Natali, L. D. Buda, U. Ebels, A. Lebib, Y. Chen, and K. Ounadjela, J. Appl. Phys. **91**, 7343 (2002).
[18] R. L. Compton and P. A. Crowell, Phys. Rev. Lett. **97**, 137202 (2006).
[19] F. G. Aliev, J. F. Sierra, A. A. Awad, G. N. Kakazei, D. S. Han, S. K. Kim, V. Metlushko, B. Ilic, and K. Y. Guslienko, Phys. Rev. B **79**, 174433 (2009).
[20] M. J. Donahue and D. G. Porter, "OOMMF User's Guide, Version 1.0," *Interagency Report NISTIR 6376*, (National Institute of Standards and Technology, Gaithersburg, MD, 1999).
[21] A. Hubert and R. Schäfer, *Magnetic Domains* (Springer, Berlin, Heidelberg, New York, 1998), p. 696.
[22] R. McMichael and M. Stiles, J. Appl. Phys. **97**, 10J901 (2005).
[23] See Supplemental Material at http://link.aps.org/supplemental/10.1103/PhysRevB.84.144406 for Videos 1–3, time dependent variation of the M_x component of magnetization corresponding to the modes 2–4 (1035 × 20nm Py dot).
[24] J. M. Winter, Phys. Rev. **124**, 452 (1961).
[25] J. C. Slonczewski, J. Magn. Magn. Mater. **31–34**, 663 (1983).
[26] K. Y. Guslienko, S. O. Demokritov, B. Hillebrands, and A. N. Slavin, Phys. Rev. B **66**, 132402 (2002).
[27] K. Y. Guslienko, J. Nanosci. Nanotechn. **8**, 2745 (2008).
[28] S. S. P. Parkin, M. Hayashi, and L. Thomas, Science **320**, 190 (2008).